

Rotation sets for networks of circle maps

Kamlesh Parwani and Krešimir Josić

Department of Mathematics
University of Houston
Houston TX 77204-3008, USA

December 14, 2005

Abstract

We consider continuous maps of the torus, homotopic to the identity, that arise from systems of coupled circle maps and discuss the relationship between network architecture and rotation sets. Our main result is that when the map on the torus is invertible, network architecture can force the set of rotation vectors to lie in a low-dimensional subspace. In particular, the rotation set for an all-to-all coupled system of identical cells must be a subset of a line.

1 Introduction

Coherent behavior in networks of coupled systems is of fundamental importance in many branches of science and engineering. The interplay between network architecture (topology) and the internal properties of network elements shape such network behavior. We show that the network architecture alone can have a strong impact on the dynamic patterns exhibited by the constituent elements. In particular, in networks of coupled circle maps architecture can force the “frequencies” of certain constituent elements to be equal, regardless of their internal dynamics. These observations are directly applicable when constructing models of networks that exhibit multirhythmic behavior or certain patterns of synchrony.

The individual cells in a dynamically evolving network are frequently observed to undergo coherent behavior. Such behavior can take different

forms ranging from synchrony and phase locking [1, 2], to reliably recurring complex patterns of activity [3, 4]. Network architecture plays a significant role in determining the type of behavior a network can exhibit [5, 6, 7], and numerical and experimental studies have shown that there is frequently a relationship between network architecture and function [8, 9].

There is a significant amount of literature on the emergence of coherent behavior in networks of interacting, continuous time dynamical systems [1]. The relation between the structure and dynamics of a network can be approached in different ways. Methods of statistical mechanics have been applied in the analysis of large networks [10], while dynamical systems and singular perturbation theory have been employed to explain the behavior of networks of small to intermediate size [11, 12]. More recently, a model independent theory of network dynamics has been proposed [13, 14], and it is the later approach that will be followed in the present work.

While most of the current literature involves continuous time systems, models of natural phenomena that are discrete in time are also frequently useful. Networks of coupled circle maps are among the most common type of such models and include pulse coupled systems [15, 16] such as neuronal networks [17] and cardiac pacemaker cells [18]. Since a discrete time dynamical system can exhibit more complex behavior than a continuous time system evolving in the same phase space, coherent behavior in such networks needs to be investigated separately.

The goal of this work is to show that the dynamics is strongly impacted by network architecture (topology). To quantify the relation between architecture and dynamics we will use rotation vectors [19], which generalize the rotation numbers of circle maps [21, 22]. The rotation number of a circle map can be thought of as a discrete time counterpart of a frequency. Similarly the components of a rotation vector can be thought of as “frequencies” of the individual cells composing a network.

We consider maps homotopic to the identity on tori that arise from systems of coupled circle maps and discuss the relationship between network architecture and rotation sets. Our main result is that the architecture of the network can force the set of rotation vectors to lie in a low-dimensional subspace. As a consequence, when the architecture of the network is such that two cells in the network *coevolve*, the corresponding components of the rotation vector, *i.e.* the “frequencies” of the two cells, must be equal. A particularly striking example of such behavior occurs in networks of identical, all-to-all coupled systems: regardless of the internal dynamics of the

constituent cells, the rotation set is at most one dimensional. Therefore, the “frequencies” of all cells must be equal. The upper semicontinuity of the rotation set implies that these results are stable under small perturbations. Consequently, all-to-all coupled networks with small inhomogeneities can be expected to exhibit frequency locking between all cells in the network. Some of these results generalize those of [23], where the networks represent coupled systems of differential equations.

The paper is organized as follows. In Section 2 we provide several examples to illustrate the impact of architecture on the structure of the set of rotation vectors. In Section 3, we consider continuous maps of tori into themselves which are homotopic to the identity and review the theory of rotation vectors and rotation sets. Then in Section 4 we show that the existence of certain subspaces that are invariant under the *backward* image of the map forces the rotation set to lie in these backward invariant subspaces. Finally, in Section 5, we prove that network architecture can imply the existence of subspaces that are invariant under the *forward* image of the map. Therefore, network architecture can force the rotation set to lie in certain low-dimensional subspaces when the map is invertible. In particular, for an all-to-all coupled network of identical cells the rotation set must be a subset of a line.

2 Examples

A coupled cell network is a coded directed graph where each node symbol represents a phase variable, and each arrow symbol represents a type of coupling. Each coupled cell network has an associated set of admissible systems of differential equations and maps. The precise relation is described in [13, 23], but, roughly speaking, each arrow ending at cell i in the graph is represented as an input in the equation that describes the evolution of that cell, and different arrows represent different types of inputs.

In this section we present examples which illustrate how network architecture can restrict the dynamics of networks of phase oscillators and circle maps. The primes in the following discussion will denote either the next iterate in the case of a discrete dynamical system, or the derivative in the case of a continuous one. We denote the n -torus by \mathbf{T}^n . As will be shown similar relations between architecture and the dynamics exist in both types of systems.

Example 2.1 Consider the network of two identical, identically interacting cells

$$\begin{aligned}\theta'_1 &= f(\theta_1, \theta_2) \\ \theta'_2 &= f(\theta_2, \theta_1),\end{aligned}\tag{2.1}$$

where $\theta_1, \theta_2 \in \mathbf{T}^1$. In the discrete case we have $f : \mathbf{T}^2 \rightarrow \mathbf{T}^1$, while for a continuous time case $f : \mathbf{T}^2 \rightarrow \mathbf{R}^1$. We will use $\theta' = f_1(\theta)$, where $\theta = (\theta_1, \theta_2)$ as shorthand. Whether equation (2.1) represents a system of differential equations or a discrete dynamical system, the circle or diagonal $\delta_{1,2} = \{(\theta_1, \theta_2) \in \mathbf{T}^2 \mid \theta_1 = \theta_2\}$ is forward invariant. The diagonal $\delta_{1,2}$ lifts to the set of diagonals $\mathcal{D}_{1,2} = \{(x_1, x_2) \in \mathbf{R}^2 \mid x_1 = x_2 + i \text{ for } i \in \mathbf{Z}\}$ in the plane and there exists a lift F_1 of (2.1) to \mathbf{R}^2 which leaves all diagonals in $\mathcal{D}_{1,2}$ invariant. Note that this lift is not unique; for all integers k , the lift $F_1 + (k, k)$ leaves the diagonals in $\mathcal{D}_{1,2}$ invariant.

In the continuous case, this implies that the lift of any orbit must be trapped between the lifts of $\delta_{1,2}$, as illustrated in Fig. 1. Therefore, if we observe the number of full oscillations that cell 1 undergoes in a given time interval, it will differ from the number of full oscillations of cell 2 by at most 1. It now follows that the difference of the average number of oscillations for the two cells converges to zero as the length of the time interval goes to infinity. This is discussed in detail in [23], which also contains many examples for the continuous case.

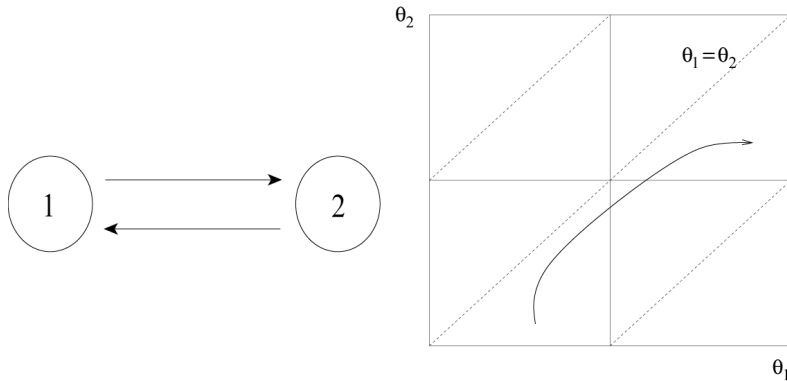


Figure 1: (Left) A network of two identical cells. (Right) The invariant circle $\theta_1 = \theta_2$ in \mathbf{T}^2 lifts to the diagonal $x_1 = x_2$ and its translates in \mathbf{R}^2 (dotted lines).

A similar conclusion holds when (2.1) represents a discrete dynamical system. The diagonal $\delta_{1,2}$, and its lift $\mathcal{D}_{1,2}$ are *forward* invariant. If the system is invertible, then the diagonals are backward invariant as well. As in the continuous case, there is a lift which leaves the diagonals $\mathcal{D}_{1,2}$ invariant, and then any lifted orbit of system (2.1) in \mathbf{R}^2 must be trapped between two diagonals in $\mathcal{D}_{1,2}$. We will show in Section 4 that the rotation set for this lift is forced to lie in the diagonal passing through zero. Since the components of the vectors in the rotation set can be thought of as a discrete time counterpart of oscillation frequencies, the difference between the “frequencies” of the two cells is zero.

Example 2.2 We next consider the following example of a network of 3 coupled circle maps:

$$\begin{aligned}\theta'_1 &= \theta_1 + \alpha \sin(2\pi\theta_1) + \beta \cos(2\pi\theta_2) + \gamma \sin(2\pi\theta_3) \\ \theta'_2 &= \theta_2 + \alpha \sin(2\pi\theta_2) + \beta \cos(2\pi\theta_1) + \gamma \sin(2\pi\theta_3) \\ \theta'_3 &= \theta_3 + \alpha \sin(2\pi\theta_3) + \beta \cos(2\pi\theta_2) + \gamma \sin(2\pi\theta_1).\end{aligned}\tag{2.2}$$

This network is depicted in Fig. 2. We will use $\theta' = f_2(\theta)$, where $\theta = (\theta_1, \theta_2, \theta_3)$, and $f_2 : \mathbf{T}^3 \rightarrow \mathbf{T}^3$ as shorthand for equations (2.2). It is easy to check directly that the subspaces $\delta_{1,2} = \{\theta \in \mathbf{T}^3 \mid \theta_1 = \theta_2\}$ and $\delta_{1,3} = \{\theta \in \mathbf{T}^3 \mid \theta_1 = \theta_3\}$ are forward invariant for the system (2.2). Moreover, for α, β , and γ sufficiently small this map is invertible, and so, $\delta_{1,2}$ and $\delta_{1,3}$ are also backward invariant.

To characterize one aspect of the dynamical system (2.2), we consider the *rotation vector*

$$\rho(x) = \lim_{n \rightarrow \infty} \frac{F_2^n(x) - x}{n},\tag{2.3}$$

where F_2 is a lift of f_2 to \mathbf{R}^3 that fixes the planes in $\mathcal{D}_{1,2}$ and $\mathcal{D}_{1,3}$. As we will show subsequently, while this limit may not exist for all points, it does exist for almost all points for any f_2 -invariant measure on \mathbf{T}^3 . When the limit exists, component i of $\rho(x)$ measures the average “advance” of cell i over one iteration. It can therefore be thought of as a discrete counterpart of frequency.

A particular example is shown in Fig. 3 for system (2.2), with $\alpha = 1/(400\pi)$ and $\beta = \gamma = 1/(150\pi)$. We will show that since the tori $\delta_{1,2}$ and $\delta_{1,3}$ are backward invariant, the regions between the lifts of the invariant tori $\delta_{1,2}$ and $\delta_{1,3}$ are invariant under the action of F_2 . This will imply that all

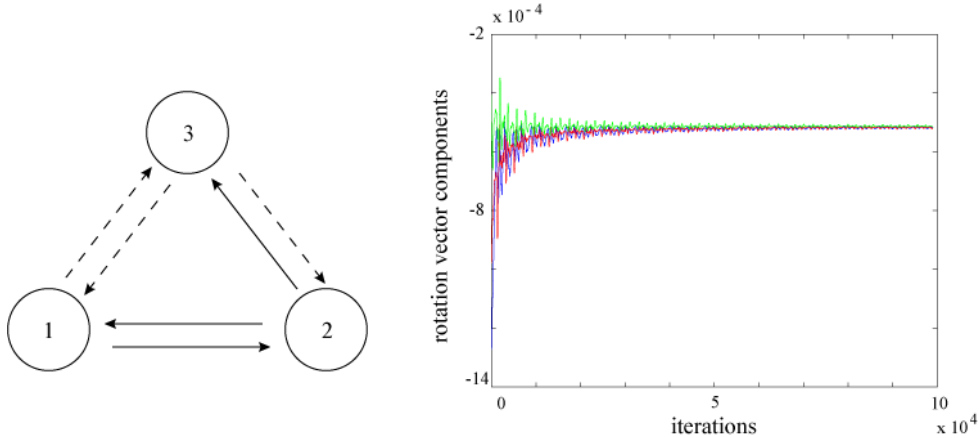


Figure 2: (Left) The 3-cell network corresponding to (2.2). (Right) The three components of the vector $(F_2^n(x) - x)/n$ as a function of n for $\alpha = 1/(400\pi)$, $\beta = \gamma = 1/(150\pi)$, and the initial condition $(0.85, 0.48, 0.90)$. Note that all components converge to the same value.

components of the rotation vector $\rho(x)$, whenever the limit exists, are equal. Furthermore, the rotation set (defined in Section 3) with respect to F_2 is forced to lie in the diagonal passing through zero.

Example 2.3 Consider the following network of 4 coupled circle maps

$$\begin{aligned}
 \theta'_1 &= \theta_1 + \alpha \cos(2\pi\theta_1) + \beta(\sin(2\pi\theta_4) + \sin(2\pi\theta_2)) \\
 \theta'_2 &= \theta_2 + \alpha \cos(2\pi\theta_2) + \beta(\sin(2\pi\theta_1) + \sin(2\pi\theta_3)) \\
 \theta'_3 &= \theta_3 + \alpha \cos(2\pi\theta_3) + \beta(\sin(2\pi\theta_2) + \sin(2\pi\theta_4)) \\
 \theta'_4 &= \theta_4 + \alpha \cos(2\pi\theta_4) + \beta(\sin(2\pi\theta_3) + \sin(2\pi\theta_1)).
 \end{aligned} \tag{2.4}$$

This architecture of this network is depicted in Fig. 4. It is easy to check directly that the subspaces $\delta_{1,3} = \{\theta \in \mathbf{T}^4 \mid \theta_1 = \theta_3\}$ and $\delta_{2,4} = \{\theta \in \mathbf{T}^4 \mid \theta_2 = \theta_4\}$ are forward invariant for the system 2.4. Again, for α and β sufficiently small, this map is invertible and then $\delta_{1,3}$ and $\delta_{2,4}$ are also backward invariant.

We will show that there exists a lift for which $\rho_1(x) = \rho_3(x)$ and $\rho_2(x) = \rho_4(x)$, when the rotation vector exists. Therefore, the “frequencies” of the pairs 1,3 and 2,4 are equal. Furthermore, the rotation set in this case lies in the plane defined by the equations $x_1 = x_3$ and $x_2 = x_4$. Fig. 4 is generated by considering an appropriate lift that fixes the codimension-one hyperplanes in $\mathcal{D}_{1,3}$ and $\mathcal{D}_{2,4}$, with $\alpha = 1/(500\pi)$ and $\beta = 1/(150\pi)$.

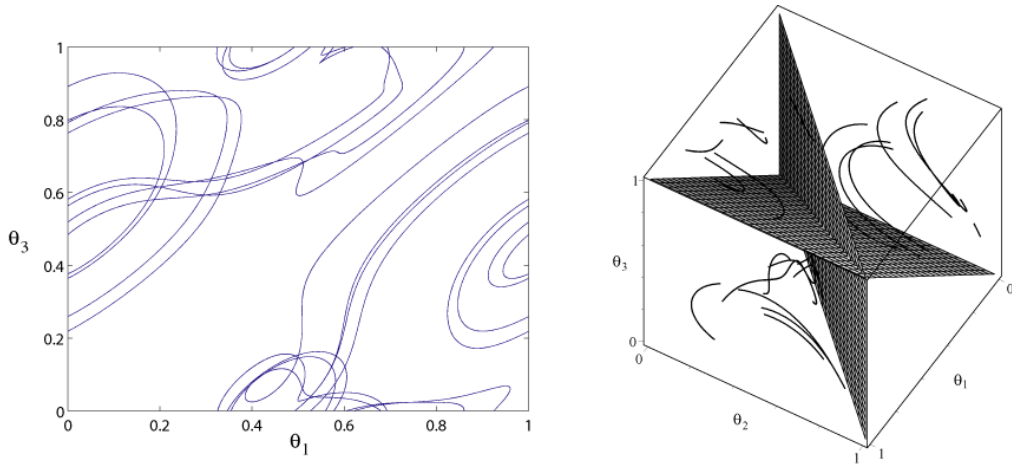


Figure 3: For the system (2.2), a projection of the orbit of $(0.85, 0.48, 0.90)$ to the θ_1, θ_3 plane (Left), and the image of the orbit in \mathbf{T}^3 (Right), together with the invariant tori $\delta_{1,2}$ and $\delta_{1,3}$.

Example 2.4 Another example that frequently appears in practice is that of an all-to-all coupled system of N identical oscillators

$$\theta'_i = f(\theta_i, \overline{\theta_1, \theta_2, \dots, \theta_N}). \quad (2.5)$$

Here the over bar means that the system is symmetric under the interchange of any two cells. It is easy to check that the diagonal $\delta_{i,j} = \{\theta \in \mathbf{T}^N \mid \theta_i = \theta_j\}$ is invariant for any $1 \leq i < j \leq N$ (see [23]). As in the previous examples, the set of codimension-one hyperplanes $\mathcal{D}_{i,j} = \{x_i = x_j + l \text{ for } l \in \mathbf{Z}\}$ is forward invariant, and if f is invertible, they are also backward invariant. We will see that this implies that all components of a rotation vector must be equal.

Example 2.5 We will show that the equality of the components of the rotation vector in the previous examples relies on the fact that certain polydiagonals (subspaces) are *backward* invariant. We now observe that, while network architecture may imply forward invariance of these polydiagonals, it may not imply equalities between the components of the rotation vector if the network equations are not invertible. Consider the following two-cell

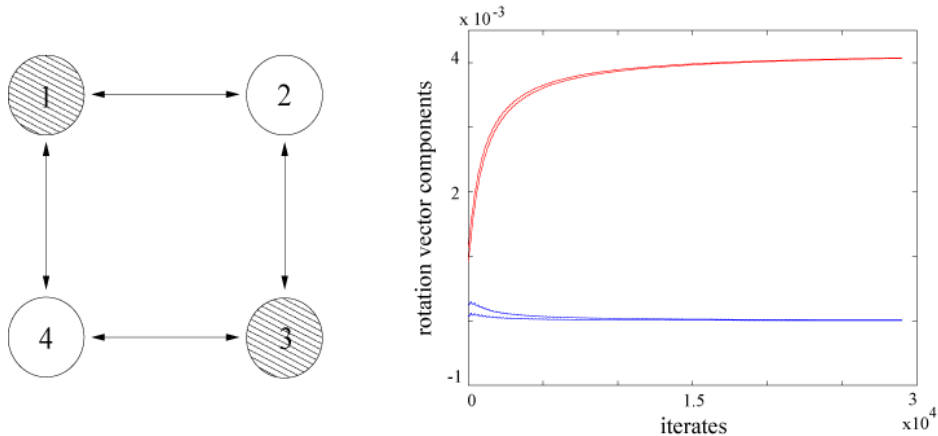


Figure 4: (Left) The 4 cell network corresponding to (2.4). (Right) The four components of the rotation vector $\rho(x)$ for the initial condition $(0.5, 0.2, 0.9, 0.5)$. Pairs of components corresponding to the average frequencies of the cells in the network with the same shading converge to the same value.

system whose architecture is shown in Fig. 1 (Left)

$$\begin{aligned}\theta'_1 &= \theta_1 + \alpha \sin(8\pi\theta_1) + \sin(2\pi\theta_2) \\ \theta'_2 &= \theta_2 + \alpha \sin(8\pi\theta_2) + \sin(2\pi\theta_1).\end{aligned}\tag{2.6}$$

For $\alpha = 1/(8\pi)$ system (2.6) is not invertible, and in particular, the $\delta_{1,2}$ circle is forward invariant but not backward invariant. We again use $\theta' = f_5(\theta)$ with $\theta = (\theta_1, \theta_2)$ as shorthand for equations (2.6). Let F_5 be the lift of f_5 to the plane which leaves forward invariant the set $x_1 = x_2$ and fixes the point $(0, 0)$. Then the i -th iterates of F_5 , for $i > 0$, satisfy $F_5^i(0, \frac{1}{4}) = (i, \frac{1}{4})$, $F_5^i(0, \frac{3}{4}) = (-i, \frac{3}{4})$, and $F_5^i(0, 0) = (0, 0)$. This implies that the average motion of the point $(0, \frac{1}{4})$ is one unit to the right, the average motion of $(0, \frac{3}{4})$ is one unit to the left, and the point $(0, 0)$ is fixed. In other words, $\rho(0, \frac{1}{4}) = (1, 0)$, $\rho(0, \frac{3}{4}) = (-1, 0)$, and $\rho(0, 0) = (0, 0)$. These are three non-collinear vectors, and so, the set of rotation vectors is not contained in a line; furthermore, the discussion in the next section implies that the rotation set must be two dimensional since it is always a convex set. Also, Fig. 5 shows that the components ρ_1 and ρ_2 of the rotation vector for the orbit starting at $(0.8, 0.49)$ do not appear to converge to the same value. This is numerical evidence supporting the fact that the rotation set for the lift F_5 does not lie

in the diagonal $x_1 = x_2$.

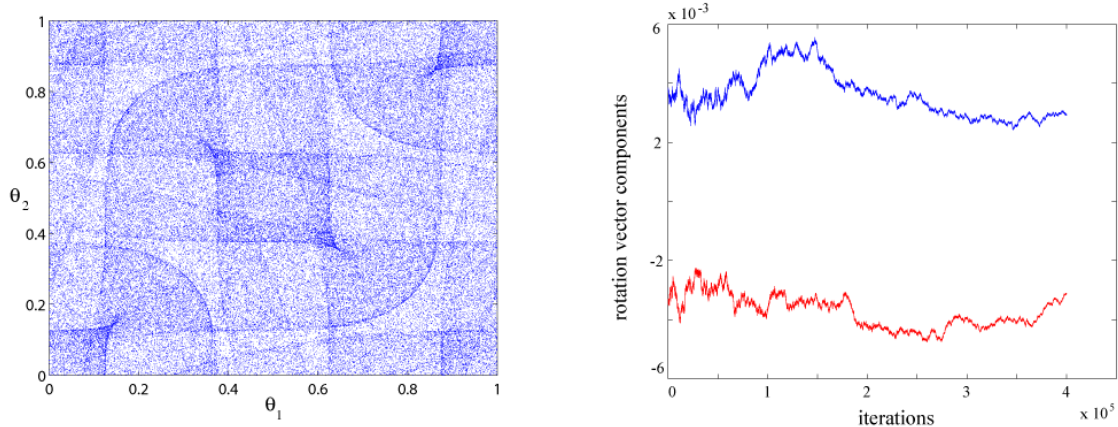


Figure 5: The orbit of the point $(0.8, 0.49)$ (Left), and the two components of the rotation vector (Right).

3 Rotation sets

To extend the results of [23] to networks of circle maps, we first review the notion of *rotation vectors* and *rotation sets*; these will play the role that “frequencies” did in the case of phase oscillators. We are interested in rotation vectors and rotation sets of $\mathbf{T}^N = \mathbf{R}^N/\mathbf{Z}^N$, the N -dimensional torus, associated to continuous maps from the torus into itself which are homotopic to the identity. We will use f to denote such a map of \mathbf{T}^N to itself and F will be a lift of f to the universal cover \mathbf{R}^N .

For the special case of homeomorphisms and \mathbf{T}^1 , Poincaré defined the rotation number associated to a lift F as $\lim_{n \rightarrow \infty} \frac{F^n(x) - x}{n}$ [21, 22]. In this case, he showed that the limit exists and is equal for all $x \in \mathbf{R}$. However, this famous result does not hold in higher dimensions and even fails to hold for degree-one, continuous maps from the circle to itself; the limits for different points may be different and the limit may not even exist for some or most points. So a natural generalization of Poincaré’s definition of rotation number would be a set of rotation vectors—the set of all limits for convergent sequences $\frac{F^n(x) - x}{n}$, for $x \in \mathbf{R}^N$. Note that even though $\lim_{n \rightarrow \infty} \frac{F^n(x) - x}{n}$ may not exist for $x \in \mathbf{R}^N$, there always exist subsequences with convergent limits

and it would be useful to include these limits in the set of rotation vectors. So we define $\rho_p(F)$ —the *pointwise rotation set of F* —as the set of limits of all convergent subsequences

$$\left(\frac{F^{n_i}(x) - x}{n_i} \right)_{i=1}^{\infty}, \text{ for } x \in \mathbf{R}^N \text{ and } n_i \rightarrow \infty. \quad (3.7)$$

We define other related sets which are associated to the set of f -invariant measures. Define $\phi : \mathbf{T}^N \rightarrow \mathbf{R}^N$ by $\phi(\theta) = F(x) - x$, where x is a lift of θ . Since $F(x + \vec{v}) = F(x) + \vec{v}$ for all $\vec{v} \in \mathbf{Z}^N$, ϕ is well defined; however, ϕ depends on the choice of the lift to \mathbf{R}^N . Now let M_e be the set of all ergodic f -invariant measures, and define the *ergodic rotation set of F* as the set of all ergodic averages with respect to ϕ by

$$\rho_e(F) = \left\{ \int \phi d\mu_e, \text{ for all } \mu_e \in M_e(f) \right\}.$$

Now let $\mu_e \in M_e(f)$, let θ be a typical point in $\text{supp}(\mu_e)$, let x be a lift of θ , and then apply the Birkhoff Ergodic Theorem to obtain

$$\int \phi d\mu_e = \lim_{n \rightarrow \infty} \frac{1}{n} \sum_{i=0}^{n-1} \phi \circ f^i(\theta) = \lim_{n \rightarrow \infty} \frac{F^n(x) - x}{n}.$$

It follows that $\rho_e(F) \subset \rho_p(F)$. This definition of the ergodic rotation set may be easily generalized by replacing f -invariant ergodic measures by f -invariant measures. Let $M(f)$ be the set of all f -invariant probability measures and define the *measure rotation set of F* by

$$\rho_{\text{mes}}(F) = \left\{ \int \phi d\mu, \text{ for all } \mu \in M(f) \right\}.$$

The Birkhoff Ergodic Theorem applied to this situation shows that

$$\int \phi d\mu = \int \left(\lim_{n \rightarrow \infty} \frac{1}{n} \sum_{i=0}^{n-1} \phi \circ f^i \right) d\mu.$$

So the rotation vector exists for μ -almost every point and $\int \phi d\mu$ is the expected value of rotation vectors with respect to the measure μ . It is clear that $\rho_e(F) \subset \rho_{\text{mes}}(F)$. It is also true that $\rho_p(F) \subset \rho_{\text{mes}}(F)$ (see [19]), that is,

if $\lim_{n_i \rightarrow \infty} \frac{F^{n_i}(x) - x}{n_i}$ exists for some $x \in \mathbf{R}^k$, then there exists an f -invariant measure μ such that $\int \phi d\mu = \lim_{n_i \rightarrow \infty} \frac{F^{n_i}(x) - x}{n_i}$. This fact follows from the following deeper result established in [19]— $\text{Conv}(\rho_p(F)) = \text{Conv}(\rho_e(F)) = \rho_{\text{mes}}(F)$, where Conv stands for the convex hull. The set $\rho_{\text{mes}}(F)$ is always a closed, convex set, while $\rho_p(F)$ does not enjoy these properties; it is not closed, open, or even connected in general. We will therefore consider $\rho_{\text{mes}}(F)$ as the most suitable generalization of Poincaré’s definition of rotation number for circle homeomorphisms homotopic to the identity. Note that this also M. Herman’s definition of the rotation set in [20].

Remark 3.1 If F and F' are two different lifts of f to \mathbf{R}^N , then $F' = F + \vec{v}$, where $\vec{v} \in \mathbf{Z}^N$. This shows that $\rho_p(F') = \rho_p(F) + \vec{v}$, which implies that $\rho_{\text{mes}}(F') = \rho_{\text{mes}}(F) + \vec{v}$. So the rotation set for a particular lift determines the rotation set for any other lift up to a translation.

Remark 3.2 We may similarly define the rotation set for a flow f_t on \mathbf{T}^N by considering a particular lift of this flow F_t on \mathbf{R}^N . Let the pointwise rotation set— $\rho_p(F_t)$ —be the collection of all limits for convergent subsequences of the following sequences:

$$\left(\frac{F_{t_i}(x) - x}{t_i} \right)_{i=1}^{\infty}, \text{ where } x \in \mathbf{R}^N \text{ and } t_i \rightarrow \infty. \quad (3.8)$$

Now we may take the convex hull of $\rho_p(F_t)$ as before. It is useful note that the set $\rho_p(F_t)$ is equal to $\rho_p(F_1)$, where F_1 is the time-one map of the flow F_t . This fact is a direct consequence of the continuity of the flow. Suppose that $\lim_{i \rightarrow \infty} \frac{F_{t_i}(x) - x}{t_i}$ exists for some $x \in \mathbf{R}^N$ and $t_i \rightarrow \infty$. Let n_i be smallest integer greater than or equal to t_i , and consider the n_i -th iterate of the time-one map $F_1^{n_i} = F_{n_i}$. Observe that $|F_{t_i}(x) - F_{n_i}(x)|$ is bounded because the torus is compact and the flow is continuous. Now it easily follows that

$$\lim_{i \rightarrow \infty} \left(\frac{F_{t_i}(x) - x}{t_i} - \frac{F_{n_i}(x) - x}{n_i} \right) = 0, \quad (3.9)$$

which implies that $\rho_p(F_t) = \rho_p(F_1)$. Therefore the results for continuous maps in this paper apply to case of flows as well.

4 Coevolving maps

In this section we introduce the notion of coevolving maps on \mathbf{T}^N and show that coevolution imposes restrictions on the dimensionality of the rotation set.

Let f be a continuous map homotopic to the identity from \mathbf{T}^N to itself as before. We will use S to denote a finite collection of $(N - 1)$ -dimensional subspaces in \mathbf{R}^N which can be defined by linear equations with coefficients in the integers—so S is the union of hyperplanes defined as $\{x \in \mathbf{R}^N \mid p_i x_i + q_j x_j = 0\}$, where p_i and q_j are integers. Also, unless specified otherwise, the term *invariant* in this section is to mean backward invariance, that is, invariant under the action of f^{-1} or F^{-1} .

Definition 4.1 *Let f be a continuous map homotopic to the identity from \mathbf{T}^N to itself and let S be a non-empty collection of $(N - 1)$ -dimensional subspaces in \mathbf{R}^N . Then f is said to coevolve with respect to S if there exists a lift F of f to \mathbf{R}^N for which all subspaces in S are backward invariant, that is, $F^{-1}(s) \subset s$, for each subspace $s \in S$.*

This definition is extremely useful in the sense that is easy to work with in terms of proofs. We now show that the requirement that a lift F of f to \mathbf{R}^N leaves invariant all the subspaces in S is equivalent to requiring that f leaves invariant the projections of all subspaces in S to \mathbf{T}^N . This provides another definition which is easier to work with in terms of the network architecture.

Proposition 4.2 *The map f coevolves with respect to S if and only if it leaves invariant the projections of all subspaces in S to \mathbf{T}^N .*

Proof Suppose that f coevolves with respect to S . Note that since f is homotopic to the identity, F commutes with all covering translations and F also leaves invariant all translates of the hyperplanes in S . Then it easily follows that f leaves invariant the projections of all subspaces in S to \mathbf{T}^N .

Now suppose that f is a continuous map homotopic to the identity from \mathbf{T}^N to itself which leaves invariant the projections of all the hyperplanes in S ; the projections of $(N - 1)$ -dimensional hyperplanes are $(N - 1)$ -dimensional tori. Let I be the intersection of all the subspaces in S and then let i be the projection of I onto \mathbf{T}^N ; therefore i is a f^{-1} -invariant torus in \mathbf{T}^N (here we assume that a point is the zero-dimensional torus). Then it is possible to find a lift F of f which leaves I invariant, after composing with a suitable

covering translation. Note that the covering translations are a subset of the Euclidean translations on \mathbf{R}^N , and these have the property that either a subspace is invariant under a covering translation or it is completely disjoint from its translate. It now follows that F also leaves invariant all subspaces in S since it fixes I . \square

So in Example 2.1, S is just the subspace defined by $x_1 = x_2$; in Example 2.2, S is the union of subspaces $x_1 = x_2$ and $x_1 = x_3$; in example 2.3, S is the union of $x_1 = x_3$ and $x_2 = x_4$; and in Example 2.4, S is the union of $x_i = x_j$, for all $1 \leq i, j \leq N$.

The goal of this section is to show that if f coevolves with respect to S , $\rho_{\text{mes}}(F)$ is contained in I , the intersection of all the subspaces in S . The proof relies on the following important fact from [19]—the extreme points of $\rho_{\text{mes}}(F)$ are also the extreme points of $\rho_e(F)$. We will make particular use of the following simple lemma.

Lemma 4.3 *Suppose S consists of a single hyperplane and let F be the lift of f that leaves invariant all translates of the hyperplane in S . Then the regions bounded by the translates of S are invariant under the forward iterates of F .*

Proof A point from the interior of the region or strip bounded by two translates of S cannot be mapped to any translate of S under F , because S is invariant under F^{-1} . Now since F is continuous, the strips bounded by the translates of S must remain invariant under the forward iterates of F . \square

Theorem 4.4 *Let f be a continuous map homotopic to the identity from \mathbf{T}^N to itself that coevolves with respect to S , and suppose that F is the lift of f to \mathbf{R}^N which leaves invariant all translations of the hyperplanes in S . Then $\rho_{\text{mes}}(F)$ is contained in I , the intersection of all subspaces in S .*

Proof First consider the simple case in which S just contains one hyperplane $H = \{x \in \mathbf{R}^N \mid p_i x_i = q_j x_j\}$. It suffices to show that all the extreme points of $\rho_{\text{mes}}(F)$ lie in H . Suppose that \vec{u} is an extreme point in $\rho_{\text{mes}}(F)$ which does not belong to H . Then there exists an ergodic f -invariant measure μ_e such that μ_e -a.e. point in $\text{supp}(\mu_e)$ has rotation vector equal to \vec{u} . In particular, there exists a point x in \mathbf{R}^N such that $\lim_{n \rightarrow \infty} \frac{F^n(x) - x}{n} = \vec{u}$. It follows that for n large enough, $F^n(x) - x$ is very close to $n\vec{u}$. So for n sufficiently large, the vector $F^n(x) - x$ based at x intersects some translate of the invariant hyperplane H . This implies that the strips bounded by the

translates of S are not invariant under the forward iterates of F . However, by Lemma 4.3, these strips are invariant, and this is a contradiction. This establishes that $\rho_{\text{mes}}(F)$ is contained in H .

Now the general case follows from the simple case described above. The arguments above show that $\rho_{\text{mes}}(F)$ belongs to each invariant hyperplane in S , and therefore, $\rho_{\text{mes}}(F)$ belongs to the intersection I . \square

Remark 4.5 Suppose that f coevolves with respect to S , where S only contains the hyperplane $\{x \in \mathbf{R}^N \mid x_i = x_j\}$, and there exists some periodic orbit for the map f . Then the projections of the rotation vector of this periodic point onto x_1 and x_2 axes must be equal. More, generally, the projection of the expected value of rotation vectors for any given f -invariant measure onto the x_1 and x_2 axes must be equal. So if we just focus our attention onto the projections of points to the circles on \mathbf{T}^N which correspond to the x_1 and x_2 axes, then the average behavior of the projections of typical points with respect to any invariant measure to these circles is identical.

Note that Theorem 4.4 above implies that in Example 2.1, there exists a lift for which the rotation set must be a subset of the diagonal since S is just $x_1 = x_2$; in example 2.2, there is a lift for which the rotation set is again a subset of the diagonal since the intersection of the planes $x_1 = x_2$ and $x_1 = x_3$ is the diagonal $x_1 = x_2 = x_3$; in Example 2.3, there exists a lift for which the rotation set lies in the plane defined by $x_1 = x_3$ and $x_2 = x_4$, which is the intersection of the codimension-one hyperplanes in S ; and in Example 2.4, there exists a lift for which the rotation set lies in the diagonal, since this is an all-to-all coupled system.

Remark 4.6 We now discuss the stability of these results under small perturbations. The rotation set is upper semicontinuous in the following sense (see [19] for more details). Let \mathcal{C}_N be the space of lifts to \mathbf{R}^N of continuous functions of \mathbf{T}^N that are homotopic to the identity. Then for every $F \in \mathcal{C}_N$ and every $\varepsilon > 0$, there exists a neighborhood V of F in \mathcal{C}_N such that, for $G \in V$, $\rho_{\text{mes}}(G)$ is contained in an ε -neighborhood of $\rho_{\text{mes}}(F)$. So if f and F are as in Theorem 4.4 above, then small perturbations have rotation sets “close” to $\rho_{\text{mes}}(F)$, but the rotation set for the perturbations need not be contained in the intersection of all the subspaces in S .

However, if we assume that f and F are diffeomorphisms for which the subspaces in S are normally hyperbolic [22], then small perturbations in

the space of C^1 -diffeomorphisms will possess codimension-one, invariant submanifolds close to the subspaces in S , and then all the arguments above go through. So for these perturbations, the rotation sets will be contained in the intersection of all subspaces in S .

Remark 4.7 The discussion above has been restricted to rotation vectors for typical points for an invariant measure, because rotation vectors exist for such points, or to expected values of the rotation vectors with respect to an invariant measure, which also always exist. Lemma 4.3 implies that even if the rotation vector with respect to a point does not exist, the average of the weighted difference between the coordinates goes to zero. More precisely, suppose that f coevolves with respect to S , where S contains the hyperplane $\{x \in \mathbf{R}^N \mid p_i x_i = q_j x_j\}$, let F be the lift which leaves invariant all translates of the hyperplanes in S , and let x be any point in the covering space \mathbf{R}^N . Then

$$\lim_{n \rightarrow \infty} \frac{p_i [F^n(x)]_i - q_j [F^n(x)]_j}{n} = 0,$$

where $[\cdot]_i$ and $[\cdot]_j$ are the projections onto the x_i and x_j axes respectively. This is because the strips bounded by the translates of $\{p_i x_i = q_j x_j\}$ are invariant under the forward iterates of F , and hence, $|p_i [F^n(x)]_i - q_j [F^n(x)]_j|$ is bounded. In the special case where $p_i = q_j = 1$, the average of the difference between the coordinates goes to zero.

5 Network architecture and coevolution

The results of the preceding section are independent of the assumption that the map f models the evolution of a network. We now add this assumption and show that network architecture can imply the existence of sets S with respect to which f coevolves. More precisely, we will now describe properties of network architecture that force the existence of subspaces invariant under the forward image of f . If f is invertible, these subspaces are also invariant under the action of f^{-1} , and then all the results of the previous section apply. The main result of this section is Theorem 5.8 which gives a direct relation between the network architecture and the structure of the rotation set. This extends the results of [23] to the case of coupled circle maps and explains the numerically observed behavior of networks in Section 2.

The evolution of a network of coupled circle maps with a given architecture is described by an *admissible* equation of the form $\theta' = f(\theta)$. We assume

that f is a continuous map homotopic to the identity from \mathbf{T}^N to itself and use the prime to denote an iterate of the map.

Definition 5.1 Two cells i and j in a network of circle maps *coevolve* if there exists a backward invariant torus $\delta_{i,j} = \{\theta \in \mathbf{T}^N : \theta_i = \theta_j\}$ for f , that is, $f^{-1}(\delta_{i,j}) \subset \delta_{i,j}$.

Now Proposition 4.2 implies that cells i and j coevolve if and only if there exists a lift F of f to R^N that leaves (backward) invariant the subspace $\Delta_{i,j} = \{x \in \mathbf{R}^N : x_i = x_j\}$, that is, $F^{-1}(\Delta_{i,j}) \subset \Delta_{i,j}$. This observation leads to the following simple proposition which follows immediately from Theorem 4.4.

Proposition 5.2 *If two cells i and j coevolve in a network of circle maps described by $\theta' = f(\theta)$, then there exists a lift F of f to \mathbf{R}^N for which the rotation set $\rho_{mes}(F)$ is a subset of $\Delta_{i,j}$.*

Definition 5.1 is difficult to use directly when determining if two cells coevolve or not. Corollary 5.7 provides a direct way to check precisely which cells coevolve in a given network.

Before stating this result, we first review some terminology. A *coloring* is obtained by assigning a color to each cell in the network. The *input set* $I(c)$ of a cell c is the set of all cells that are connected to c by some arrow pointing to it. To be more precise, every cell $b \in I(c)$ is identified with one arrow from b to c . The notion of a *balanced coloring* is of fundamental importance in our discussion.

Definition 5.3 A coloring (denoted by \bowtie) is *balanced* if for every pair of cells c and d with the same color there is a color preserving input isomorphism $\beta : I(c) \rightarrow I(d)$. That is, b and $\beta(b)$ have the same color and b and $\beta(b)$ are connected to c and d respectively with arrows of the same type for every $b \in I(c)$.

We forgo the formalism of [13] and resort to the following example in order to illustrate the notion of a balanced coloring.

Example 5.4 Consider the network of cells introduced in Example 2.2. Three colorings of this network are depicted in Fig. 6. The only coloring that is not balanced is the one on the right, since in this case cell 1 connects to cells 2 and 3 with arrows of different type. The input set to cell 2 consists

of cells 1 and 3, and the input set to cell 3 consists of cells 1 and 2. However the map β taking cell 1 to itself and cell 2 to cell 3 is not an input isomorphism. Another balanced coloring is obtained for this network by using the same color for all cells.

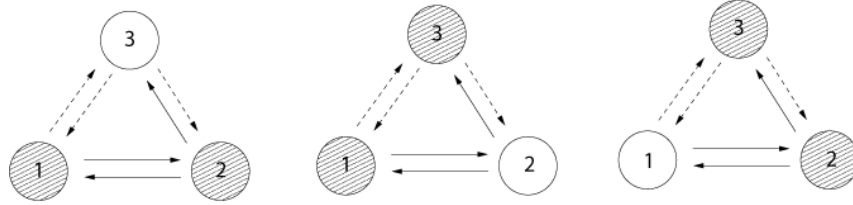


Figure 6: Different colorings of the 3-cell network corresponding to (2.2). The two colorings on the left are balanced, while the one on the right is not.

A balanced coloring \bowtie can be viewed as an equivalence relation. We write $i \bowtie j$ if the two cells i and j share the same color. There is a 1:1 correspondence between colorings and polydiagonals, where the *polydiagonal* associated to a coloring \bowtie is the subset of \mathbf{T}^N defined by

$$\delta_{\bowtie} = \{\theta \in \mathbf{T}^N : \theta_c = \theta_d \text{ whenever } c \text{ and } d \text{ have the same color}\}.$$

The polydiagonal δ_{\bowtie} is a torus in the phase space \mathbf{T}^N of the entire network with codimension equal to the number of equivalence classes defined by the coloring \bowtie . The lift Δ_{\bowtie} of δ_{\bowtie} to \mathbf{R}^N is a linear subspace.

Definition 5.5 Let \bowtie be a coloring on a coupled cell network. Then \bowtie is *robustly polysynchronous* if for every admissible map f , δ_{\bowtie} is *forward* invariant.

Now if f is invertible, \bowtie is robustly polysynchronous if and only if δ_{\bowtie} is backward invariant, and then Proposition 4.2 implies that there exists a lift F of f to \mathbf{R}^N for which Δ_{\bowtie} is (backward and forward) invariant.

The invariance of δ_{\bowtie} is, in general, a consequence of network architecture and not just the symmetries of the network [13]. The following theorem is proved for ODE's in [23] and the arguments there can be easily adapted to the setting of coupled circle maps.

Theorem 5.6 *Let \bowtie be a coloring of a network of coupled circle maps. Then \bowtie is robustly polysynchronous if and only if \bowtie is balanced.*

Proof Theorem 4.3 in [13] asserts that this theorem is valid for ODE’s on Euclidean phase space (\mathbf{R}^N). An almost identical argument establishes that this result holds for coupled maps on \mathbf{R}^N . Now the theorem for coupled circle maps essentially follows from simple “lifting and projecting” arguments.

First note that the torus $\delta_{\bowtie} \subset \mathbf{T}^N$ is forward invariant for f if and only if there exists a lift F to \mathbf{R}^N for which the polydiagonal $\Delta_{\bowtie} \subset \mathbf{R}^N$ is forward invariant. The maps F and f are admissible for the same network architectures, the only difference being the space in which the individual cells are evolving. Therefore, in this manner, a balanced coloring for a network of circle maps is a balanced coloring for the network obtained from a lift, and vice versa.

Suppose that \bowtie is a balanced coloring for the network of circle maps. There exists a lift F for which the coloring of the lifted network is also balanced. The version of Theorem 4.3 in [13] for maps on \mathbf{R}^N implies that Δ_{\bowtie} is F -invariant. By projecting to \mathbf{T}^N , we can see that δ_{\bowtie} is f -invariant. This shows that for a balanced coloring \bowtie , the torus $\delta_{\bowtie} \subset \mathbf{T}^N$ is forward invariant for any admissible map f , that is, \bowtie is robustly polysynchronous.

To prove the converse we must show that if the torus δ_{\bowtie} is forward invariant for all admissible maps on \mathbf{T}^N , then Δ_{\bowtie} is forward invariant for all admissible maps for the network on \mathbf{R}^N . In this case the version of Theorem 4.3 in [13] applicable to maps would imply that \bowtie is balanced. However, a subspace is invariant globally if it is locally invariant, and locally every admissible map is the lift of a network of circle maps (namely, the local projection of the map on \mathbf{R}^N to the torus \mathbf{T}^N), so we have the required result. \square

Next we use Theorem 5.6 to provide a simple test to determine when two cells coevolve. Given two different cells i and j , let $\bowtie_{i,j}$ be the coloring in which cells i and j have the same color and all other cells have distinct colors.

Corollary 5.7 *Suppose that a network of coupled circle maps is described by $\theta' = f(\theta)$, where f is invertible and homotopic to the identity. If the coloring $\bowtie_{i,j}$ is balanced, the two cells i and j coevolve.*

Proof Theorem 5.6 implies that the torus $\delta_{\bowtie_{i,j}} = \delta_{i,j} = \{\theta \in \mathbf{T}^N : \theta_i = \theta_j\}$ is forward invariant. Since f is invertible, $\delta_{i,j}$ is also backward invariant. It now follows that i and j coevolve. \square

We now provide a direct way of determining the structure of the rotation set.

Theorem 5.8 *Suppose that a network of coupled circle maps is described by $\theta' = f(\theta)$, where f is invertible and homotopic to the identity. If $\{\bowtie_{i_k, j_k}\}_{k=1}^n$ is collection of balanced colorings, there exists a lift F of f to \mathbf{R}^N for which $\rho_{\text{mes}}(F) \subset \bigcap_{k=1}^n \Delta_{i_k, j_k}$.*

Proof Corollary 5.7 implies that δ_{i_k, j_k} is backward invariant for f , for all k . Now apply Proposition 4.2 to obtain a lift F that leaves (backward) invariant Δ_{i_k, j_k} , for all k . By Theorem 4.4, $\rho_{\text{mes}}(F) \subset \bigcap_{k=1}^n \Delta_{i_k, j_k}$. \square

We can now fully justify the observations made in Example 2.2. As discussed in Example 5.4, the colorings $\bowtie_{1,2}$ and $\bowtie_{1,3}$ are balanced. Therefore there exists a lift F for which $\rho_{\text{mes}}(F)$ is contained in $\Delta_{1,2} \cap \Delta_{1,3}$. As a consequence, all components of any rotation vector in $\rho_{\text{mes}}(F)$ must be equal. Similarly in Example 2.3, the colorings $\bowtie_{1,3}$ and $\bowtie_{2,4}$ are balanced, and therefore, $\rho_{\text{mes}}(F) \subset \Delta_{1,3} \cap \Delta_{2,4}$.

A similar observation leads to the following corollary. This explains the examples 2.1 and 2.4 of Section 2.

Corollary 5.9 *Suppose that a network of all-to-all coupled cells is described by $\theta' = f(\theta)$, where f is invertible and homotopic to the identity. Then there exists a lift F of f to \mathbf{R}^N for which $\rho_{\text{mes}}(F)$ is a subset of the diagonal $\Delta = \{x_i = x_j \text{ for all } i, j\}$.*

Proof Since any cell receives input from all other cells in the network, any pair of cells receives input from exactly the same set of cells. Therefore, for all cells i and j , the coloring $\bowtie_{i,j}$ is balanced. By Theorem 5.8, there exists a lift F for which the rotation set is contained in the intersection of all polydiagonals $\Delta_{i,j}$, that is, $\rho_{\text{mes}}(F) \subset \Delta$. \square

Remark 5.10 If f is not invertible, cells i and j may also coevolve. However, since in this case backward invariance of $\delta_{\bowtie_{i,j}}$ under f needs to be checked directly, since it is not implied by forward invariance.

Remark 5.11 For a given network, two cells may coevolve even when $\bowtie_{i,j}$ is not balanced. However, Theorem 5.6 shows that such examples are not robust and are hence atypical.

The following Proposition provides a way of checking if $\bowtie_{i,j}$ is a balanced coloring.

Proposition 5.12 ([23]) *The coloring $\bowtie_{i,j}$ is balanced if and only if every other cell in the network connects to both cells i and j with the same number (which may be zero) of arrows of each type, and the arrows from i to j are the same in number and type as those from j to i .*

6 Conclusion

We have shown that architecture can have a significant impact on the dynamics in a network of interacting circle maps. Therefore, when using this type of network as a model, it is important to choose architectures which are able to support the desired dynamics. Similarly, if a network is known to have a certain architecture, one can conclude that certain dynamic behaviors are not possible.

We note that it does not appear that network architecture has a similar impact on other quantities that are frequently used to describe the dynamics, such as the entropy and the Hausdorff dimension of attractors. It is likely that more information about the internal dynamics of the individual cells and their interactions is necessary in order to draw any conclusions about these quantities.

Acknowledgments

This work was supported in part by NSF Grant DMS-0244529. K. Josić was also supported by NSF Grant ATM-0417867.

References

- [1] A. Pikovsky, M. Rosenblum, and J. Kurths, *Synchronization: A Universal Concept in Nonlinear Science*. Cambridge: Cambridge University Press, 2003.
- [2] Y. Kuramoto, *Chemical oscillations, waves, and turbulence*. New York: Springer-Verlag, 1984.
- [3] Y. Ikegaya, G. Aaron, R. Cossart, D. Aronov, I. Lampl, D. Ferster, and R. Yuste, “Synfire chains and cortical songs: Temporal modules of cortical activity,” *Science*, vol. 304, p. 559, 2004.

- [4] E. Izhikevich, “Polychronization: Computation with spikes.” to appear in *Neural Comp.*, 2005.
- [5] I. Vragović, E. Louis, C. Boschi, and G. Ortega, “Diversity-induced synchronized oscillation in close-to-threshold excitable elements arranged on regular networks.” Preprint, cond-mat/0410171, 2005.
- [6] G. Scheler, “Network topology influences synchronization and intrinsic read-out.” Preprint, q-bio.NC/0507037, 2005.
- [7] S. Mangan and U. Alon, “Structure and function of the feed-forward loop network motif,” *Proc. Natl. Acad. Sci. USA*, vol. 100, p. 11980, 2003.
- [8] A. A. Prinz, D. Bucher, and E. Marder, “Similar network activity from disparate circuit parameters,” *Nat. Neurosci.*, vol. 7, p. 1345, 2004.
- [9] S. Song, P. Sjöström, M. Reigl, S. Nelson, and D. Chklovskii, “Highly nonrandom features of synaptic connectivity in local cortical circuits,” *PLoS Biol.*, vol. 3, p. 0507, 2005.
- [10] R. Albert and A. Barabási, “Statistical mechanics of complex networks,” *Rev. Mod. Phys.*, vol. 74, p. 47, 2002.
- [11] F. C. Hoppensteadt and E. Izhikevich., *Weakly connected neural networks*. New York: Springer-Verlag, 1997.
- [12] J. Rubin and D. Terman, “Geometric singular perturbation analysis of neuronal dynamics,” in *Handbook of dynamical systems, Vol. 2*, pp. 93–146, Amsterdam: North-Holland, 2002.
- [13] M. Golubitsky, I. N. Stewart, and A. Török, “Patterns of synchrony in coupled cell networks with multiple arrows,” *SIAM J. Appl. Dynam. Sys.*, vol. 4, p. 78, 2005.
- [14] I. Stewart, M. Golubitsky, and M. Pivato, “Symmetry groupoids and patterns of synchrony in coupled cell networks,” *SIAM J. Appl. Dynam. Sys.*, vol. 2, no. 4, p. 609, 2003.
- [15] A. T. Winfree, *The geometry of biological time*, vol. 12 of *Interdisciplinary Applied Mathematics*. New York: Springer-Verlag, second ed., 2001.

- [16] G. Ermentrout and N. Kopell, “Multiple pulse interactions and averaging in systems of coupled neural oscillators,” *J. Math. Bio.*, vol. 29, p. 195, 2001.
- [17] M. Zeller, M. Bauer, and W. Martienssen, “Neural dynamics modelled by one-dimensional circle maps,” *Chaos Soliton Fract.*, vol. 5, no. 6, p. 885, 1995.
- [18] D. Michaels, E. Matyas, and J. Jalife, “Mechanisms of sinoatrial pacemaker synchronization: a new hypothesis,” *Circ. Res.*, vol. 61, no. 5, p. 704, 1987.
- [19] M. Misiurewicz and K. Ziemian, “Rotation sets of maps of tori,” *J. London Math. Soc.*, vol. 40, p. 490, 1989.
- [20] M. Herman, “Existence et non existence de tores invariants par des difféomorphismes symplectiques,” *Séminaire sur les Équations aux Dérivées Partielles 1987–1988*, Exp. No. XIV, 24 pp., École Polytech., Palaiseau, 1988.
- [21] A. Katok and B. Hasselblatt, *Introduction to the modern theory of dynamical systems*. Cambridge: Cambridge University Press, 1995.
- [22] C. Robinson, *Dynamical Systems: Stability, Symbolic Dynamics, and Chaos*. New York: CRC Press, 1998.
- [23] M. Golubitsky, K. Josić, and E. Shea-Brown, “Winding numbers and average frequencies in phase oscillator networks.” to appear in *J. Non-linear Sci.*, 2005.